Bogusław KAROLEWSKI
Piotr LIGOCKI

MODELLING OF LONG BELT CONVEYORS

MODELOWANIE DŁUGICH PRZENOŚNIKÓW TAŚMOWYCH*

A mathematical model that allows the analysis of the dynamic states of a belt conveyor was presented. A way of modelling wave phenomena in the tape, changes of mass and resistances to motion and elements of the drive system (motors, frequency converters, couplings, gears and co-operation between the belt and drive pulley) was briefly described. A start up of an exemplary belt conveyor was simulated with the use of obtained formulas. The start-up time histories obtained computationally were compared with measurements. The verified belt conveyor model can be utilized to examine various phenomena and operating states of a belt conveyor.

Keywords: *belt conveyor, modelling, computer simulation, dynamics, inductive drive.*

Przedstawiono matematyczny model przenośnika taśmowego umożliwiający analizę dynamicznych stanów pracy urządzenia. Skrótowo opisano sposób modelowania zjawisk falowych w taśmie, zmian mas i oporów ruchu oraz elementów układu napędowego czyli silników, przekształtników, sprzęgieł, przekładni i współpracy bębna napędowego z taśmą. Rozwiązując komputerowo uzyskane zależności, symulowano rozruch przykładowego przenośnika. Porównano przebiegi rozruchowe uzyskane obliczeniowo z pomiarowymi. Zweryfikowany model można wykorzystać do badania różnych zjawisk i stanów pracy przenośnika.

Słowa kluczowe: *przenośnik taśmowy, modelowanie, symulacja komputerowa, dynamika, napęd indukcyjny.*

1. Introduction

Belt conveyors are economical, efficient and are a more and more often used means of transportation. Advancements in belt conveyor technology have provided essentially unlimited adaptability, allowing conveyors to provide solutions for every geographic region and all belts of applications worldwide [1]. During the design and operation of longer and more efficient conveyors, new demanding problems have appeared which did not occur in shorter structures [15]. The start up of a conveyor involves significant variability of belt forces as well as strokes of driving torques and accelerations. The threat of belt damage and other subassemblies exists. Additional problems appear in the case of the curvilinear belt route [3].

Carrying out investigations on real operative installations are difficult and expensive. Moreover, results of measurements can only be utilized in the evaluation of existing objects. On this base it is not possible to determine the effects of potential changes or new solutions. The formulation of coherent mathematical models of belt conveyors which take into account phenomena that occur in dynamic states, considerably expands investigative and design possibilities and gives a chance to predict and solve various questions.

Despite many years of using conveyors, many exploitation problems have not been resolved [14]. Companies exploiting belt conveyors expect high reliability and performance to be ensured. Simulation studies using a mathematical model of the conveyor, made at the stage of design, allows this to be made and they have a significant impact on the subsequent process of exploitation and reliability. Examples of use of the model to determine dynamic waveforms in mechanical elements (speeds, accelerations, forces) is shown for example in [9], and both in mechanical and in electrical forms (currents and torques of motors) in [21, 22].

The initial stages of the development of dynamic modelling of belt conveyors is described in [11]. In the 70's at the University of Hanover, Germany, the model of the tape was divided into two sections,

taking into account the viscoelastic properties [2]. Then the model was extended, taking into account a larger number of masses [3].

In the 80's at the University of Newcastle in Australia, a model based on the propagation of stress waves in the tape was built [10]. Also, the U.S. company Conveyor Dynamics built a model that contains the source variable as a function of time, the driving force, taking into account friction and theviscoelastic properties of the tape [31].

In Poland in the 90's theoretical basis for modeling the belt and the whole conveyor was developed at the Technical University of Wroclaw [4, 17, 36, 46], Silesian University of Technology [30] and the Academy of Mining and Metallurgy in Cracow [24].

Comprehensive modelling which takes into account the transverse conveyor belt moving in a vertical direction was dealt with at the Technical University of Delft in the Netherlands [28]. Work allowing the determination of the behavior in the vicinity of the tape's horizontal curves was carried out at the Austrian University of Mining and Metallurgy in Leoben [8]. The company Krupp Fördertechnik and the University of Hanover focused especially on modelling the drive [39, 40]. The created model provides the ability to dynamically calculate the convergence side tape on horizontal curves.

Most of these centers still improve old models [3, 12, 21, 22, 25, 29]. Chinese centers also carry out such work [9].

The use of multiple drives in long conveyors entails new challenges and problems, such as inelastic slip on one of the pulleys and different distribution of power between the drives. Work regarding these issues include [16, 33, 37, 42].

A new theme is to study possible energy savings [23, 26, 38, 44].

Many authors dealing with the behavior of a model study of conveyor belt dynamic states, expanded the model in the desired direction, focusing on the improvement of a particular item of equipment, while ignoring or assuming a simplified description of other phenomena. In a large part of these works motor models were greatly simplified (for example, the course of the motor torque was approximated with two straight sections), which can result in large differences between the

behavior of the model in relation to the actual device. In none of these works (apart from the works carried out by the authors of this article [17, 18, 20–22]) changes in the parameters of induction motors are not taken into account.

In the study, the results of which can be found in the literature, little attention was given to modelling the mechanical connection of the motor shaft drive drum. Even in many of the advanced models of conveyor there was a simplification assumed, consisting of the treatment of the clutch and mechanical gear as rigid elements. When the flexible coupling was taken into account [30], models of other elements were simplified.

There is no fully comprehensive approach where different elements and events would be described in a similar way. Electricians favor the problem of modeling motors, simplifying the mechanical issues, and the mechanics behave vice versa.

In addition to models arising in scientific centers, there are solutions created by companies designing conveyors, but they do not give details of used dependence.

So work began on the creation of an extensive conveyor model that takes into account:
- ring and squirrel cage motors with parameters changing as a result of displacement of current and core saturation,
- frequency converters and soft-start circuits,
- flexibility of flexible couplings and clutch slip,
- mechanical deflection of gear teeth,
- the possibility of the belt slipping on the drive pulley,
- one-, two- or three pulley drive and indirect drives,
- different models of belt, which can be divided into any number of segments,
- excavated material weight changes as a result of charging and discharging,
- changes of resistance to motion as a function of the mass, velocity and force of the strip,
- components resistance of motion connected with pressing of the belt in idlers or deformation of the belt and excavated material between idler sets and traditionally accepted idlers rolling resistance and slipping of the belt on idlers,
- gradually moving the belt and changing the value of the friction coefficients of static to dynamic,
- impact of belt sag between idler sets and transverse forces in the belt to vibration in the vertical plane.

The presented model was created by combining the well-known mathematical descriptions of various conveyor components, the use of the research results of its subassemblies and taking into account the theoretical analysis. Without detailed research it is difficult to assess which elements have a significant impact on the behavior of the system. Therefore, attempts were made to take into account in the model as much as possible phenomena occurring in the real device. Conveyor components were described in a uniform convention with a similar degree of accuracy. After verification of the model, it is then possible with its use, to study the impact of various phenomena and parameters on the obtained waveforms. These tests can be used to formulate simplified versions of the general model, dedicated to specific, narrowly focused goals.

2. The belt Conveyor Model

The functioning of every conveyor element (represented in fig. 1) is described with the use of a mathematical relationship remaining in a uniform convention to ensure the possibility of complex solving received equations. A block diagram of a drive system model connected with a single motor as well as a block diagram of the overall belt conveyor model is presented in figures 2 and 3.
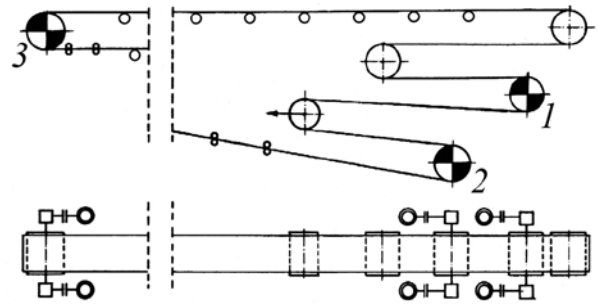

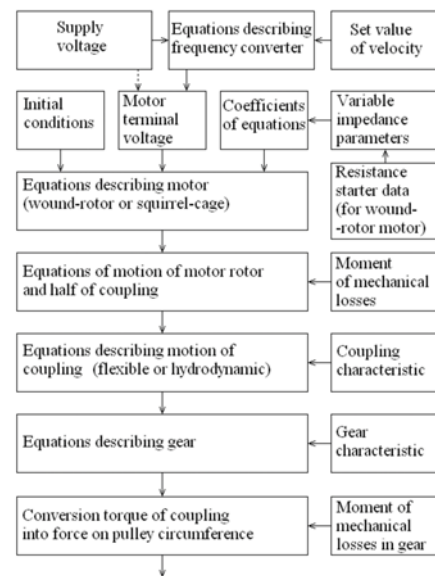Fig. 1. Belt conveyor system with marked numbers of drive pulleys

Fig. 2. Block diagram of a single drive system model

2. 1. The belt Model

The most important part of the conveyor is a rubber belt. The belt movement is described by two partial differential equations, of which one represents the equilibrium of the forces acting on the belt and the other the relationship between the stress and elongation of the belt [45]. The models section of the belt may have a different number of elements. The simplest model is elastic. A more powerful model is the two-element model of Kelvin-Voigt, consisting of springs and a damper connected in parallel. The three element model is seen as standard. It is made as a serial connection between the spring and Kelvin-Voigt model. Even more powerful is the four element model.

Each model can be completed with a module with Coulomb friction by taking into account changes in friction. The coefficient of friction that occurs in the formulas on resistances to the motion section of the belt changes from static to dynamic. When a section of the belt starts moving, the ratio decreases from static value μ_s to movement μ_r. Further growth of some components of motion resistances with speed increases must be reflected by calculating these resistances. By taking into consideration the impact of Coulomb friction, from a one-element model, a two-parameter model is achieved, and from a two-element model a three-parameter model is achieved , etc. [28, 31, 46]. Therefore, a distinction between the number of elements and the number of model parameters was introduced.

There were tests carried out which presented how the choice of rheological model of the belt influences the obtained dynamical proc-
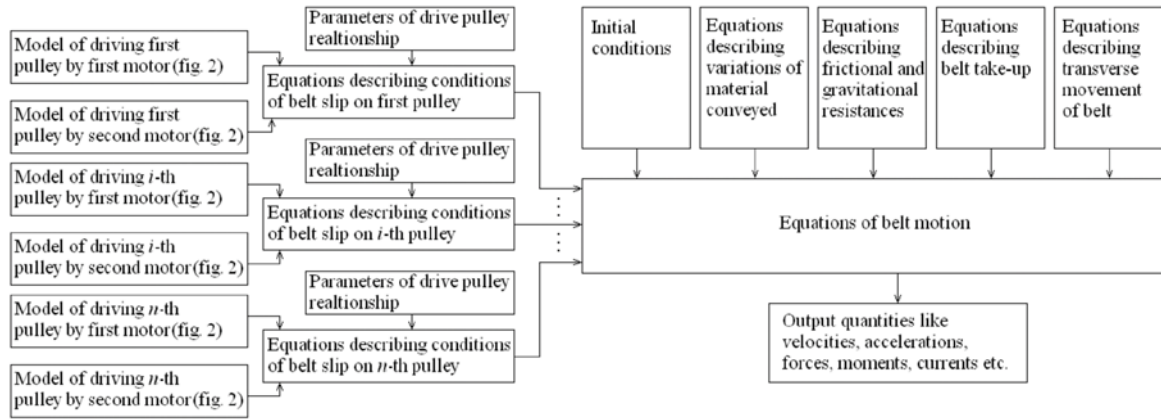
Fig. 3. Block diagram of the mathematical model of a belt conveyor

esses. By using the developed conveyor model, starting waveforms were calculated.

The calculations were made for the conveyor system shown in figure 1, with a length of 3620 meters, equipped with a steel cord belt with a width of 1.8 m and nominal speed 5.24 m/s. The drive consisted of five ring induction motors with a power of 630 kW each and a rated voltage of 6 kV, coupled with three drum drives (two in front and one at the end). The effect of using the 1, 2 and 3-element belt model, which includes changes of friction, making the model to be 2, 3 and 4-parameters, on strength waveforms in the belt which tensions the drum was examined. The results – the top three waveforms in Figure 4 – were compared with the results of measurements carried out by the staff of the Institute POLTEGOR [35] (lower course). Parameters for each model should be selected so that they correspond to the approximation of the same creep curve. Due to this, the dissimilarity between the characteristics are caused by the differences between models, and not by differences in parameter values.
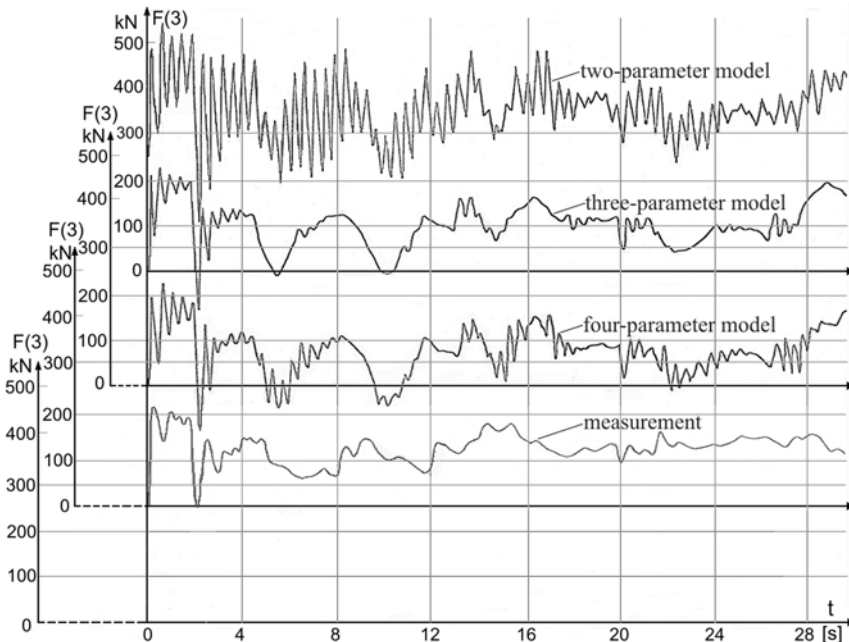
three-parameter model (two-elements with variable friction). Some differences are mainly caused by a slightly different frequency of vibration force in calculations and measurements. This may be due to inaccurate estimation of the belt load factor during the measurements. Adding springs to the four parameter model resulted in the generation of additional vibration which did not occur in the measured waveform. A similar effect can be expected in the case of a five-parameter model. Models with greater than 4 parameters are rarely used and have not been studied.

In most tasks it is enough to use the two-element model including a variable friction, that is three-parameters. This model was used in further studies. A high impact on the quality of the results is the appropriate selection of the variables in the model. Parameters of models for transient analysis to be determined in a specific way so as to ensure that approximating the measured waveforms in the time duration of the transient, that is up to periods of tens of seconds. It is possible to use the free vibration tape sample analysis method [45].

2. 2. Mass calculation

In the mass of a particular segment, the influence of idler inertias or non-drive pulleys (converted into equivalent mass), as well as masses of the belt and load, were taken into account.

An exemplary formula which determines the mass of the *i*-th segment of the upper strand is:

$$m(i) = \left(m_{jt} + m_{jn}(i) + \frac{4 \cdot z_{kg} \cdot J_{kg}}{l_{zg}(i) \cdot D_{kg}^2} \right) \cdot l(i) \quad [kg] \quad (1)$$

where:

m_{jt}	– belt mass per unit length [kg·m^{-1}],
$m_{jn}(i)$	– load mass per unit length on the belt segment between *i* and *i+1* point [kg·m^{-1}],
$l(i)$	– length of *i*-th segment [m],
z_{kg}	– number of rolls in each upper idler rolls station,
J_{kg}	– roll moment of inertia [kg·m^2],
$l_{zg}(i)$	– idler rolls stations spacing for upper strand [m],
D_{kg}	– idler diameter for upper strand [m].

Fig. 4.   Comparison of the forces in the belt on the take-up pulley obtained using different models of the belt with the measurement results

Vibration forces obtained with the 2-parameter model possess too large an amplitude and are insufficiently suppressed. The most similar to the measuring results are the results of the application of the

The mass of belt segments on drive pulleys depends on conditions of cooperation between the belt and pulley. If the belt has the same velocity as a pulley's lining, masses of the pulley and other elements which are connected with it in a rigid way (i.e. slow-speed wheels of toothed gear) will also be taken

into account in calculations (fig. 5). Masses of further elements of the drive system (following wheels of toothed gear, couplings, motor rotors) are connected in a flexible way. Their motion is described by applying other equations. If the belt starts to slip on the pulley's lining, the motion of the pulley and part of the gear should also be described by applying a separate equation.
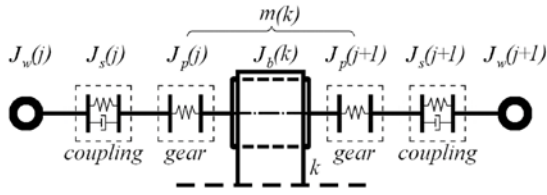

Fig. 5. Drive system connected with k-th drive pulley: m(i) – mass of segment on drive pulley, moments of inertia of: $J_w(j)$- j-th motor rotor, $J_s(j)$- j-th coupling, $J_p(j)$- j-th gear, $J_b(k)$- k-th drive pulley

The load level of the upper strand can change. The model enables the simulation of conveyor start-up with a belt that is unloaded (empty), fully loaded or loaded in a specified degree. There is a possibility to simulate the start-up of a conveyor included in a sequence of conveyors, that is preceded by an earlier conveyor which drops a load onto the conveyor (fig. 6).

Dropping a load from the belt on the head station causes the emptying of the following belt segments (area $n_{pz} - n_{pl}$), whereas the feeding conveyor fills the terminal segments from loading point n_{pl}. Variability of the mass and load distribution along the carry strand are functions of the belts' velocities of both the examined and feeding conveyor. Differences of moments of switching on of the conveyors and duration of each start-up were taken into account.
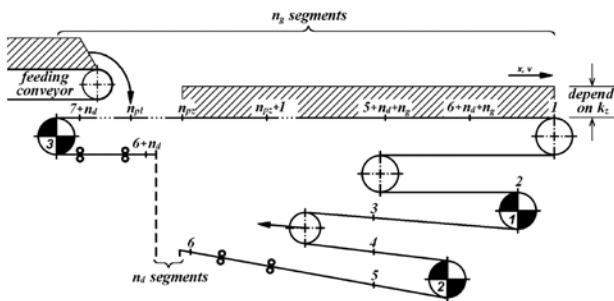

Fig. 6. Scheme of load distribution on the conveyor belt

2. 3. Resistance of motion variability

The motion of the belt is opposed by motion resistances W. Both passive resistances involving friction forces and active gradient resistance connected with downhill or uphill haulage were taken into consideration. A method of elementary resistances [43] and its modifications [4, 5, 6, 7] are used in the model with the aim of determining friction resistances. The resistance of motion components such as resistance of the idler bearing rolls rotation W_{tk} [27] and resistance of belt slipping on idlers surface W_{st} [43] are taken into account. Moreover, the trampling resistance [13], that is compounded of indentation rolling resistance W_{tt} [4, 41], flexing belt resistance W_{pt} and flexing material resistance W_{du} is taken into account:

$$W = f(W_{tk}, W_{st}, W_{tt}, W_{pt}, W_{du}) \text{ [N]} \qquad (2)$$

and:

$$W_{tk} = f(m, v, T) ,$$
$$W_{st} = f(m, v) ,$$
$$W_{tt} = f(m) ,$$
$$W_{pt} = f(m, v, F) ,$$
$$W_{du} = f(m, v, F) .$$

where: m – mass on given belt segment [kg],
  v – belt velocity [m·s^{-1}],
  T – ambient temperature [°C],
  F – belt force [N].

Example calculations were performed for the conveyor with the parameters given in section 2.1.

Dynamical changes of values of particular components of primary motion resistances of the belt during start-up were determined. Examinations for two variants according to the used way of motion resistances modelling were performed:
  – variant I – using method of elementary resistances,
  – variant II – using method of calculation of the components of a belt conveyor flexure resistance.

Courses of the actual values of particular components of primary resistances of motion of the whole belt for variant I during a period of start-up which last for 60 s, are presented in fig. 7.
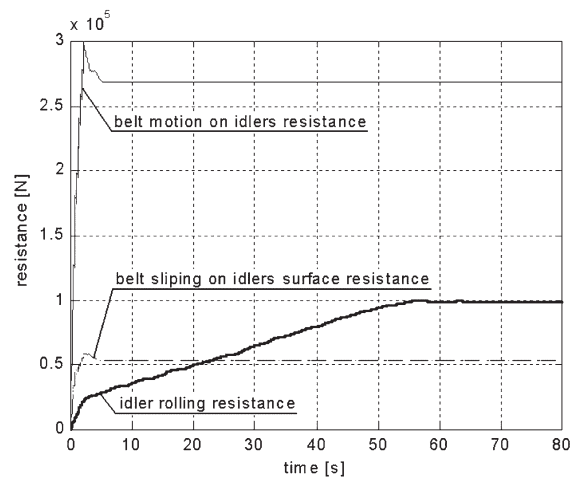

Fig. 7. Courses of actual values of particular components of belt primary motion resistances during start-up determined by the method of elementary resistances

At the beginning of start-up all the resistances increase from zero in connection with the gradual start of the moving of subsequent segments of the flexible belt. The further slow increase of idler rolling resistances results from their dependence on belt velocity. Belt slipping and motion resistances have the highest values at the moment when the whole belt starts moving. When the belt velocity increases, friction factors decrease from static to dynamic value and therefore both these resistances have lower values. The belt slipping on idler surface resistances and belt motion on idler resistances depend on the quality of conformance and the parameters of the belt which are invariable during the start-up period. Futhermore, they depend on the stage of belt loading which is only variable on short segments of the conveyor. Therefore in further parts of start-up, after the first several-seconds of the period of changes, these resistances only changed insignificantly.

In fig. 8 courses of changes of primary motion resistance components achieved in variant II which means taking into consideration the resistances dependence on belt tension are presented.
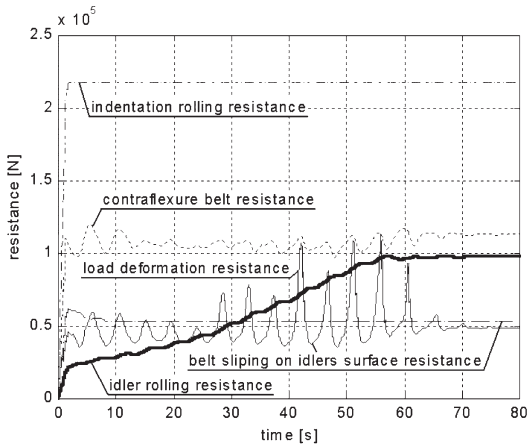
Fig. 8. Courses of actual values of particular components of belt primary motion resistances during start-up determined by method of calculation of the components of a belt conveyor flexure resistance

In calculations using the method of calculation of the components of a belt conveyor flexure resistance two analogical components occur like in the method of elementary resistances. They are idler rolling resistance and belt slipping on idlers surface resistance. For both variants the same formulas describing these two components were applied. Therefore both shapes of courses as well as values of these two components in both variants are very similar, which is visible in fig. 6 and 7. Strictly speaking, slight vibration appeared in the idlers rolling resistance. Small differences are also connected with a tiny extension of starting time in variant II.

Belt motion on idler resistance that is presented in variant I was replaced by flexure resistance in variant II shattered into three differential components. Except in the period of initial increase, indentation rolling resistance (fig. 8) is in fact invariable. However, in courses of contraflexure belt resistances and even more of load deformation resistances, oscillations connected with dependence of these resistances on belt tension occur.

The courses of sum of belt primary motion resistances for both variants are presented in fig. 9.
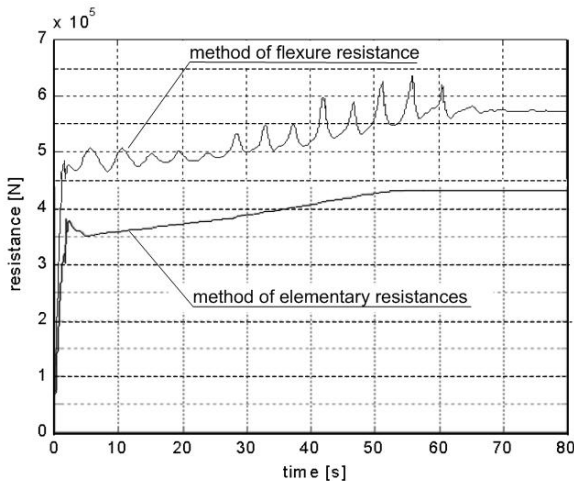

Fig. 9. Courses of sum of belt primary motion resistances during start-up calculated for both methods

At the beginning of start-up the value of sum of resistances increases suddenly in connection with the gradual start in the movement of following belt segments. This phenomenon is partly compensated by higher values of static resistances during transition from static

to dynamic friction at the moment of the start in the movement of following segments. In the further part of the course, the resistance increases, together with a velocity, until the belt achieves a steady velocity.

Values of resistances corresponding to particular phases of motion in variant II are much higher than in variant I. This explains the fact, that when used in the model of the conveyor method of elementary resistances, underrate values of currents drawn by the motors are obtained [20]. In further studies, the method of the components of a flexure resistance was used.

2. 4. Model of the belt sag

Except for longitudinal oscillations, transverse displacement of the belt as belt sag between adjacent idler stations is taken into account in the model. Examination of the belt sag effect is aimed at preventing the appearance of the belt lifting above idlers within concave curves in a vertical plane during dynamic states (fig. 10). Curves along the conveyors route are applied in order to limit ground works costs.
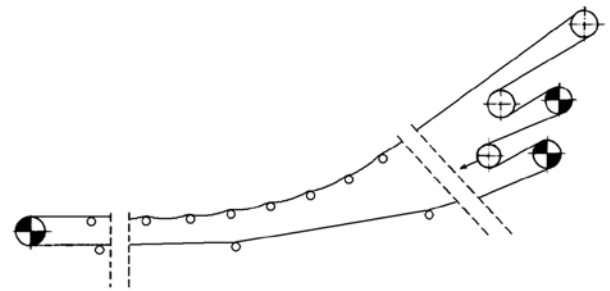

Fig. 10. Model of belt sags between idlers within conveyor route concave curves in a vertical plane

Based on the catenary equation, belt sag f is expressed as follows:

$$f = \frac{l_z^2 \cdot G}{8F} \ [\text{m}] \tag{3}$$

where: l_z – length between adjacent idler stations [m],
F – horizontal component of force acting on a belt segment between idler stations [N],
G – weight per unit of belt and load [N·m^{-1}].

2. 5. Model of conveyors drive

In the conveyor belt model, circuit models of driving induction motors, both wound-rotor and squirrel-cage, were utilised.

The form of flux equations is as follows:

$$\frac{d}{dt}\psi_{s1} = u_{l1} - \frac{R_l + R_s}{L_l + L_{sz}}\psi_{s1} + \frac{R_l + R_s}{L_z}[\cos\vartheta_e \cdot \psi_{r1} + \cos(\vartheta_e + 120°) \cdot \psi_{r2} + \cos)\vartheta_e - 120°) \cdot \psi_{r3}] \ [\text{V}]$$

$$\frac{d}{dt}\psi_{s2} = u_{l2} - \frac{R_l + R_s}{L_l + L_{sz}}\psi_{s2} + \frac{R_l + R_s}{L_z}[\cos(\vartheta_e - 120°) \cdot \psi_{r1} + \cos\vartheta_e \cdot \psi_{r2} + \cos(\vartheta_e + 120°) \cdot \psi_{r3}] \ [\text{V}]$$

$$\psi_{s3} = -\psi_{s1} - \psi_{s2} \ [\text{Wb}] \tag{4}$$

$$\frac{d}{dt}\psi_{r1} = \frac{R_r}{L_z}[\cos\vartheta_e \cdot \psi_{s1} + \cos(\vartheta_e - 120°) \cdot \psi_{s2} + \cos(\vartheta_e + 120°) \cdot \psi_{s3}] - \frac{R_r(L_l + L_{sz})}{L_{rz}(L_l + L_{sz}')} \cdot \psi_{r1} \ [\text{V}]$$

$$\frac{d}{dt}\psi_{r2} = \frac{R_r}{L_z}[\cos(\vartheta_e + 120°) \cdot \psi_{s1} + \cos\vartheta_e \cdot \psi_{s2} + \cos(\vartheta_e - 120°) \cdot \psi_{s3}] - \frac{R_r(L_l + L_{sz})}{L_{rz}(L_l + L_{sz}')} \cdot \psi_{r2} \ [\text{V}]$$

$$\psi_{r3} = -\psi_{r1} - \psi_{r2} \ [\text{Wb}]$$

current equations:

$$i_{s1} = \frac{1}{L_l + L_{sz}} \psi_{s1} - \frac{1}{L_z}[\cos\vartheta_e \cdot \psi_{r1} + \cos(\vartheta_e + 120°) \cdot \psi_{r2} + \cos(\vartheta_e - 120°) \cdot \psi_{r3}] \ \ [A]$$

$$i_{s2} = \frac{1}{L_l + L_{sz}} \psi_{s2} - \frac{1}{L_z}[\cos(\vartheta_e - 120°) \cdot \psi_{r1} + \cos\vartheta_e \cdot \psi_{r2} + \cos(\vartheta_e + 120°) \cdot \psi_{r3}] \ \ [A]$$

$$i_{s3} = -i_{s1} - i_{s2} \ \ [A] \tag{5}$$

$$i_{r1} = -\frac{1}{L_z}[\cos\vartheta_e \cdot \psi_{s1} + \cos(\vartheta_e - 120°) \cdot \psi_{s2} + \cos(\vartheta_e + 120°) \cdot \psi_{s3}] + \frac{L_l + L_{sz}}{L_{rz}(L_l + L_{sz}')} \cdot \psi_{r1}$$

$$i_{r2} = -\frac{1}{L_z}[\cos(\vartheta_e + 120°) \cdot \psi_{s1} + \cos\vartheta_e \cdot \psi_{s2} + \cos(\vartheta_e - 120°) \cdot \psi_{s3}] + \frac{L_l + L_{sz}}{L_{rz}(L_l + L_{sz}')} \cdot \psi_{r2}$$

$$i_{r3} = -i_{r1} - i_{r2} \ \ [A]$$

The following electromagnetic moment formula and equation of motion was assumed

$$T_e = -\frac{2}{3} p \cdot L_M[(i_{s1} \cdot i_{r1} + i_{s2} \cdot i_{r2} + i_{s3} \cdot i_{r3}) \cdot \sin\vartheta_e + (i_{s1} \cdot i_{r2} + i_{s2} \cdot i_{r3} + i_{s3} \cdot i_{r1}) \cdot \sin(\vartheta_e + 120°)$$
$$+ (i_{s1} \cdot i_{r3} + i_{s2} \cdot i_{r1} + i_{s3} \cdot i_{r2}) \cdot \sin(\vartheta_e - 120°)] \ [N \cdot m]$$

$$\frac{d\Omega_e}{dt} = \frac{p}{J}(T_e - T_m) \ \ [rad \cdot s^{-2}] \tag{6}$$

$$\frac{d\vartheta_e}{dt} = \Omega_e \ \ [rad \cdot s^{-1}] \tag{7}$$

where:

$\psi_{s1}, \psi_{s2}, \psi_{s3}$ – actual values of stator fluxes [Wb],

$\psi_{r1}, \psi_{r2}, \psi_{r3}$ – actual values of rotor fluxes converted into stator [Wb],

i_{s1}, i_{s2}, i_{s3} – actual values of stator currents [A],

i_{r1}, i_{r2}, i_{r3} – actual values of rotor currents converted into stator [A],

u_{l1}, u_{l2} – actual values of the supplying line phase voltages [V],

R_s, R_r – stator and rotor resistances converted to the stator side [Ω],

R_l, L_l – resistance and inductance of the motor supplying line [Ω], [H],

L_z, L_{sz}' – substitute inductance and stator transient inductance [H],

ϑ_e, Ω_e – „electrical" angle between axes of the first stator and rotor phase in the modelled motor with pole pairs number of $p = 1$ and „electrical" value of rotor 's angular velocity [rad], [rad·s^{-1}],

T_e – electromagnetic torque acting on the motor's rotor with pole pairs number of p [N·m],

T_m – sum of motor mechanical losses torque and the torque transferred via coupling connected with the motor [N·m],

J – inertia of spinning masses connected rigidly with the rotor [kg·m^2],

t – time [s].

The variability of motor parameters caused by current displacement and saturation was taken into account. Each drive in the program was modelled independently.

2. 6. Modelling of frequency converters and soft start equipment

Squirrel cage motors can be supplied by frequency converters. A model of frequency converter with bipolar pulse-width modulation with the assistance of carrying a signal was applied [32]. Each of the conveyor squirrel-cage driving motors may be supplied via a frequency converter with a scalar control of velocity, according to the principle of control that assumes stabilization of voltage amplitude with

stator flux [34]. There is a possibility to assume an arbitrary shape of the start-up ramp in the program.

The model takes into account the possibility of supplying drive motors with soft-start devices. To this end, during the simulation ignition time of the suitable thyristor in each half-period of voltage was determined, thus changing the value of the effective voltage.

2. 7. Modelling of driving torque transmission systems

Elasticity of gears, flexibility of flexible couplings and slip of hydrodynamic couplings are taken into account [18]. Characteristics of each flexible coupling is approximated as:

$$T_c = a\Delta\phi + b\Delta\phi^3 + \tau_s(a + 3b\Delta\phi^2)\frac{d\Delta\phi}{dt} \ \ [N \cdot m] \tag{8}$$

where: T_c – moment transmitted via coupling [N·m],

$\Delta\varphi$ – torsional angle measured between coupling's elements [rad],

a, b – factors which determine participation of linear and nonlinear term of an equation in couplings characteristics [N·m ·rad^{-1}], [N·m ·rad^{-3}]

τ_s – delay time, i.e. time-constant of torsional angle growing after step change of torsional moment [s].

2. 8. Belt slip of drive pulley

The driving force that is delivered to the drive pulley is transmitted to the belt by means of the friction effect [19, 46]. If the force winding on drive pulley is too high in relation to the value of the force winding off drive pulley, the belt will be too weakly pressed against the pulley and a belt slip will appear. The occurrence of inelastic belt slip phenomena is undesirable. One should then choose preliminary values of belt forces or use the starting torque control to prevent the belt slip. The conveyors model involves the belt slip effect and it permits the determination of velocity difference between the belt and the pulley.

The maximal value of the force which can be transmitted from a drive pulley to the belt is determined as [19]:

$$PD(k) = F(i+1) \cdot (e^{\mu \cdot \alpha} - 1) + W(i) + m(i) \cdot \frac{dv(i)}{dt} \ \ [N] \tag{9}$$

where: $PD(k)$ – driving force which can be transmitted to the belt without belt slip [N],

$F(i+1)$ – force in the belt winded off the drive pulley [N],

μ – factor of friction between the belt and the drive pulley,

α – pulleys wrapping angle [rad].

If the force on the circumference of the drive pulley is smaller than the maximal force, which the pulley can transmit to the belt, then all the force, produced by driving motors and transferred to the pulley's circumference, will be transmitted to the belt. If the abovementioned condition isn't fulfilled then the force transmitted to the belt via the drive pulley will only be equal to the maximum force possible to transfer. It is expressed by the following equations:

$$P_b = \begin{cases} PS & \text{for} \quad PS \leq PD \ \text{and} \ v_{po\acute{s}} = 0, \\ PD & \text{in other cases} \end{cases} \ \ [N]$$

$$v_{po\acute{s}} = v_b - v(i), \quad [m \cdot s^{-1}] \tag{10}$$

$$\frac{d}{dt} v_{po\acute{s}} \cdot l(i) \cdot [m(i) - m_{jt}] = PS - P_b \ \ [N]$$

where: P_b – driving force transmitted to the belt via drive pulleys [N],

PD – maximal force possible to transmit to the belt by drive pulley [N],

PS – force on the circumference of the drive pulley, originated from driving motors [N],

$v(i)$ – belt velocity in point of winding on the pulley [m·s^{-1}],

v_b – linear velocity of points on pulleys circumference [m·s^{-1}],

v_{pos} – rubbing speed between belt and drive pulley [m·s^{-1}].

A surplus of driving moment accelerates the drive pulley. The belt slip then appears between the pulley and the belt. When the surplus of driving moment fades, the belt catches up with the pulley and the belt slip disappears.

3. Measuring verification

Simulation program was developed to solve the model. The program enables the simulation of diverse operating conditions of a conveyor and the investigation of the influence of particular phenomena on obtained courses of forces, moments, velocities, accelerations, voltages, currents and powers absorbed by driving motors.

The measuring verification was performed by matching selected computational and measured time histories. The measurement was made on a 3620 meter long conveyor described in section 2.1 [35]. The conveyor was driven by five wound-rotor motors, 630 kW each, connected with three drive pulleys. The take up device was operated periodically, ensuring 228 kN of belt pretension.

Analysis was carried out for start up time courses of belt forces at points near the take-up pulley, velocities at points near the first head drive pulley and for a current of one of the driving motors for cases when the belt is loaded at 33% (fig. 11, 12 and 13) and 75% (fig. 14 and 15) of nominal value. Computational time histories are slightly different than results of measurement but the character of changes is similar which reflects the correctness of the model. Maximal differences between instantaneous values from computations and measurement for forces do not exceed 30% of the measured value. Differences for currents do not exceed 27% of the rated current of motor (75 A). Velocities differ no more than about 7% of steady velocity. The maximal differences are often achieved once, after the appearance of a step in the course of given quantity. In most parts of the start-up period differences are much smaller. Bearing in mind how many elements and phenomena influence results, the obtained accuracy of computations seems to be satisfactory.
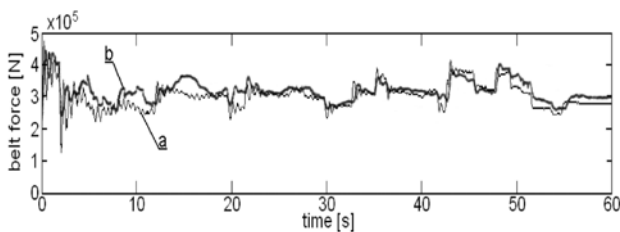

Fig. 11. *Time histories of belt forces on take-up pulley (33% of belt load): a) computation, b) measurement*

4. Summary

The conveyor model is a universal tool which can be utilised to optimize conveyor operation, check new solutions or to verify a project. Tests performed during the design of the conveyor allows parameters to be properly chosen. This has an important impact on the exploitation and reliability of the work of the device.The simulation program based on the model can be applied to determine the ways of
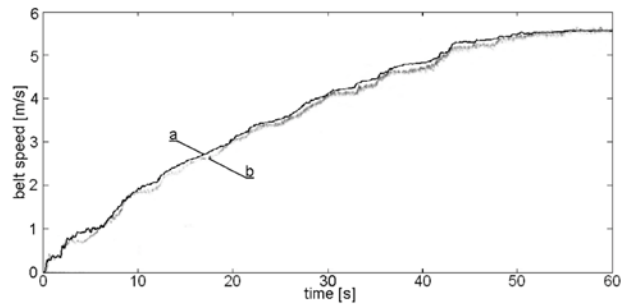

Fig. 12. *Time histories of belt velocities near head station(33% of belt load): a) computation, b) measurement*
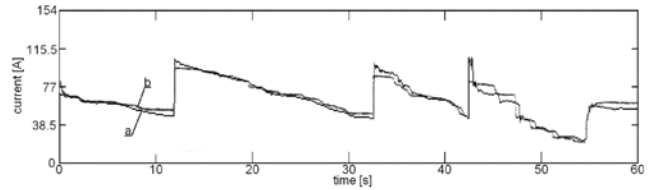

Fig. 13. *Time histories of starting current of motor driven pulley No 2 (33% of belt load): a) computation, b) measurement*
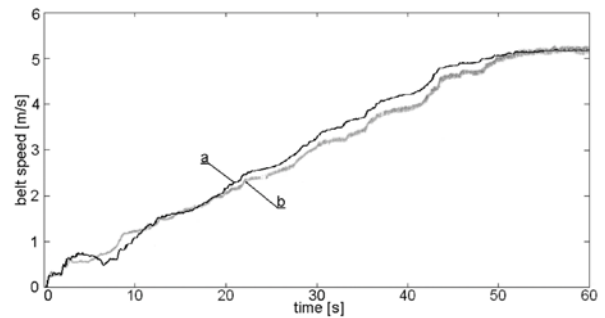

Fig. 14. *Time histories of belt velocities near head station (75% of belt load): a) computation, b) measurement*
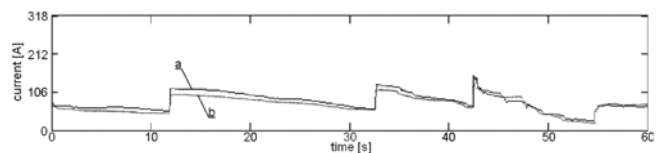

Fig. 15. *Time histories of starting current of motor driven pulley No 2 (75% of belt load): a) computation, b) measurement*

controlling driving systems which ensure limitation of critical mechanical quantities in the system's elements, especially values of the belt forces in dynamic states. The model enables the examination of, among others, the influence of drive location, time of start of particular motors, kind of motors' selection, way of control of frequency converters for squirrel-cage motors or selection of resistance starters and program of start-up control for wound-rotor motors. The criterion of start-up control assessment is to achieve the shortest possible start-up duration with assurance of not exceeding the specified belt forces level. The control of steady work should ensure such a belt velocity control that will maintain the nominal level of belt load, regardless of the value of the fed material stream.

References

1. Continental Group of Companies, Advantages Offered by Belt Conveyor Technology. Bulk Solids Handling 2001, Vol. 21; 2: 183–187.
2. Funke H. Zum dynamischen Verhalten von Förderbandanlagen beim Anfahren und Stillsetzen unter Berücksichtigung der Bewegungswiderstände. Ph.D. Dissertation 1973, Hannover University of Technology, Germany.
3. Funke H, Hartmann K, Lauhoff H. Design and Operating Performance of a Long-Distance Belt Conveyor System with Horizontal Curves and Simultaneous Material Transport in the Upped and Lower Strands. Bulk Solids Handling 2000, Vol. 20; 1: 45–55.
4. Gładysiewicz L. Die Ermittlungsmethode des Eindruckrollwiderstandes zwischen Fördergurt und Tragrolle. Wrocław: Prace Naukowe Instytutu Górnictwa Politechniki Wrocławskiej 1983; 42: 58–70.
5. Gładysiewicz L. Metoda wyznaczania oporów głównych przenośnika taśmowego ze szczególnym uwzględnieniem właściwości taśmy. Prace Naukowe Centralnego Programu Badań Naukowych 02.05., Praca habilitacyjna 1990, Warszawa: Wydawnictwo Politechniki Warszawskiej.
6. Gładysiewicz L. Metoda obliczeń składowych oporu falowania przenośnika taśmowego. Górnictwo Odkrywkowe 1993; 2: 30–42.
7. Gładysiewicz L, Król R, Bukowski J. Eksperymentalne badania oporów ruchu przenośnika taśmowego (Tests of Belt conveyor resistance to motion). Eksploatacja i Niezawodnosc – Maintenance and Reliability 2011; 3: 17–25.
8. Grimmer KJ, Kessler F. The Design of Belt Conveyors With Horizontal Curves. Bulk Solids Handling 1992, Vol. 12: 4: 557–563.
9. Guangbu Li, Ruqiong Li. Belt Conveyor Modelling and Performance Simulation Based on AMESim. Materials of Second International Conference on Information and Computing Science 2009: 304–307.
10. Harrison A. Criteria for Minimizing Transient Stresses in Conveyor Belts. Transactions Institute Engine Australia, Mechanical Engineering 1983, Vol. 8; 3: 129–134.
11. Harrison A. Belt Conveyor Research 1980-2000. Bulk Solids Handling 2001, Vol. 21; 2: 159–164.
12. Harrison A. Non-linear Belt Transient Analysis by Numerical Simulation. Bulk Solids Handling 2008;4: 242–247.
13. Jonkers CO. The indentation rolling resistance of belt conveyors. Fördern und Heben1980, Vol.30; 4: 313–317.
14. Kacprzak M, Kulinowski P, Wędrychowicz D. Informatyczny system zarządzania procesem eksploatacji górniczych przenośników taśmowych (Computerized information system used for management of mining belt conveyors operations). Eksploatacja i Niezawodnosc – Maintenance and Reliability 2011; 2: 81–93.
15. Kahrger R, Dilefeld M, Pohl M. Henderson 2000 – A World Class Conveying System. Bulk Solids Handling 2000, Vol. 20; 3: 319–322.
16. Karanth B, Ramakoteswara RK, Parameswaran MA. A Systematic Approach to the Experimental Investigation on Two Pulley Conveyor Belt Drive. Bulk Solids Handling 1995,Vol. 15; 4: 579–586.
17. Karolewski B. Modelowanie zjawisk dynamicznych w przenośnikach taśmowych. Wrocław: Prace Naukowe Instytutu Energoelektryki Politechniki Wrocławskiej, Praca habilitacyjna 1985; 63.
18. Karolewski B. An Investigation of Various Conveyor Belt Drive Systems Using a Mathematical Model. Bulk Solids Handling 1986, Vol. 6; 2: 349-354.
19. Karolewski B. Modell der Durchhaenge zwischen den Förderbandtragrollensaetzen und des Schlupfes auf der Antriebstrommel. Deutsche Hebe- und Fördertechnik 1992; 5: 46–50.
20. Karolewski B, Ligocki P. Modelowanie przenośnika taśmowego. Górnictwo Odkrywkowe 2004; 1: 41–45.
21. Karolewski B, Ligocki P. Modelowanie dynamiki przenośników taśmowych z silnikami indukcyjnymi klatkowymi. Przegląd Elektrotechniczny 2009; 3: 56–58.
22. Karolewski B, Ligocki P. Wpływ sposobu rozruchu na obciążenia wybranych elementów przenośnika taśmowego. Przegląd Górniczy 2010; 1-2: 33–37.
23. Kasztelewicz Z, Szymański J. Metoda energooszczędnego sterowania napędem przenośnika o regulowanej prędkości taśmy w kopalniach węgla brunatnego (Energy saving control method of electrical drives in coveyor belts with regulated speed in surface brown coal mine). Archives of Mining Sciences 2008; 53: 319–329.
24. Kulinowski P, Jabłoński R. Computer – Aided Analysis of Dynamics of Belt Conveyor With Automatic Follow-Up Device Stretching the Belt. 1-st International Conference on Information Technologies in the Minerals Industry, 1997.
25. Kulinowski P. Analiza dynamiki rozruchu przenośników taśmowych z uwzględnieniem charakterystyk sprzęgieł hydrokinetycznych. Transport Przemysłowy 2004; 1: 25–29.
26. Lauhoff H. Speed Control on Belt Conveyors – Does it Really Save Energy? Bulk Solids Handling 2005; 25(6): 368–377.
27. Lodewijks G. The Rolling Resistance of Conveyor Belts. Bulk Solids Handling 1995, Vol. 15; 1: 15–22.
28. Lodewijks G. Dynamics of Belt Systems. Delft University of Technology, The Netherlands, Ph.D. thesis 1996, Universitettsdrukkerij.
29. Lodewijks G. Two Decades Dynamics of Belt Conveyor Systems. Bulk Solids Handling 2002, Vol. 22; 2: 124–132.
30. Markusik S. Dynamika rozruchu przenośników taśmowych z napędem jedno- lub dwubębnowym czołowym. Gliwice: Zeszyty Naukowe Politechniki Śląskiej 1982; 711.
31. Nordell LK, Ciozda ZP. Transient belt stresses during starting and stopping: Elastic response simulated by finite element methods. Bulk Solids Handling 1984, Vol. 4; 1: 99–104.
32. Nowacki Z. Modulacja szerokości impulsów w napędach przekształtnikowych prądu przemiennego. Warszawa: PWN 1991.
33. Nuttal A, J, G, LodewkijS G. Dynamics of Multiple Drive Belt Conveyor Systems. Particle & Particle Systems Characterization 2007; 24: 365–369
34. Orłowska-Kowalska T. Bezczujnikowe układy napędowe z silnikami indukcyjnymi. Wrocław: Oficyna Wydawnicza Politechniki Wrocławskiej 2003.
35. Palczak Cz. i inni, Pomiary wybranych wielkości przenośnika 15.02 po okresie docierania pod obciążeniem. Prace Programu Rządowego PR8/1.2-89/R1, Wrocław: COBPGO Poltegor 1983.
36. Pieńkowski K. Modelling and digital simulation of the multimotor electromechanical system of long belt conveyors. Modelling, Simulation and Control, 1985, Vol. B5; 1: 43–63.
37. Qing He, Hong Li. Review of Dynamic Modelling and Simulation of Large Scale Belt Conveyor System, International Conference on

Intelligent Computing and Information Systems ICICIS 2011, Part 1, CCIS 134: 167–172.
38. Reicks A, V. Conveyor Models as Quantitative Platforms for Belt Conveyor Energy Options. Bulk Solids Europe 2012; 10.
39. Schulz G. Further Results in the Analysis of Dynamics Characteristics of Belt Conveyors. Bulk Solids Handling 1993; 13(4): 705–710.
40. Schulz G. Comparison of Drives for Long Belt Conveyors. Bulk Solids Handling 1995; 15(2): 247–251.
41. Spaans C. The Calculation of the Main Resistance of Belt Conveyors. Bulk Solids Handling 1991; 11(4) 15–22.
42. Sur S. Dual Drives for Belt Conveyors. Bulk Solids Handling, August 1987; 7(4): 509–514.
43. Ścięgosz W. Obliczenia podstawowe przenośników taśmowych. Wrocław: Zeszyty Problemowe COBPGO POLTEGOR 1972; 43.
44. Zhang S, Xia X. Modelling and Energy Efficiency Optimization of Belt Conveyors. Applied Energy 2011; (88)9: 3061–3071.
45. Żur T. Viscoelastic Properties of Conveyor Belts. Bulk Solids Handling 1986; 6(3): 553–560.
46. Żur T, Hardygóra M. Przenośniki taśmowe w górnictwie. Katowice: Wyd. Śląsk 1996.

Bogusław KAROLEWSKI
Faculty of Electrical Engineering
Institute of Electrical Machines, Drives and Measurements
Wrocław University of Technology
Wybrzeże Wyspiańskiego 27, 50-370 Wrocław, Poland
E-mail: boguslaw.karolewski@pwr.wroc.pl

Piotr LIGOCKI
MT PROJEKT, s.c,
ul. Jeżowska 14, 54-049 Wrocław, Poland
E-mail: piotr.ligocki@mtprojekt.pl